

# Development of Metabolically Stable Inhibitors of Mammalian Microsomal Epoxide Hydrolase

Christophe Morisseau,<sup>†</sup> John W. Newman,<sup>†,‡</sup> Craig E. Wheelock,<sup>†,§</sup> Thomas Hill III,<sup>†</sup>  
Dexter Morin,<sup>||</sup> Alan R. Buckpitt,<sup>||</sup> and Bruce D. Hammock<sup>†,\*</sup>

Department of Entomology, U. C. Cancer Center, and Department of Molecular Biosciences, School of Veterinary Medicine, University of California, Davis, California 95616

Received December 20, 2007

The microsomal epoxide hydrolase (mEH) plays a significant role in the metabolism of xenobiotics such as polyaromatic toxicants. Additionally, polymorphism studies have underlined a potential role of this enzyme in relation to a number of diseases, such as emphysema, spontaneous abortion, eclampsia, and several forms of cancer. We recently demonstrated that fatty amides, such as elaidamide, represent a new class of potent inhibitors of mEH. While these compounds are very active on recombinant mEH *in vitro*, they are quickly inactivated in liver extracts reducing their value *in vivo*. We investigated the effect of structural changes on mEH inhibition potency and microsomal stability. Results obtained indicate that the presence of a small alkyl group  $\alpha$  to the terminal amide function and a thio-ether  $\beta$  to this function increased mEH inhibition by an order of magnitude while significantly reducing microsomal inactivation. The addition of a hydroxyl group 9–10 carbons from the terminal amide function resulted in better inhibition potency without improving microsomal stability. The best compound obtained, 2-nonylsulfanyl-propionamide, is a competitive inhibitor of mEH with a  $K_i$  of 72 nM. Furthermore, this new inhibitor significantly reduces mEH diol production in *ex vivo* lungs exposed to naphthalene, underlying the usefulness of the inhibitors described herein. These novel inhibitors could be valuable tools to investigate the physiological and biological roles of mEH.

## Introduction

Epoxide hydrolases (EH; E.C.3.3.2.3)<sup>1</sup> are important enzymes that catalyze the hydrolysis of alkene oxides and arene oxides to their corresponding dihydrodiols (1, 2). Microsomal epoxide hydrolase (mEH) is a key hepatic enzyme involved in the metabolism of numerous xenobiotics, such as polyaromatic hydrocarbons, 1,3-butadiene, phenytoin, and carbamazepine (1–3). The mEH action is a detoxification process for most of these substrates (3); however, in some cases, such as for benzo( $\alpha$ )pyrene 7,8-oxide, diol formation can lead to the stabilization of a secondary epoxide, increasing the mutagenic and carcinogenic potential of the product (4, 5). In addition to its hepatic role, mEH is likely involved in the extrahepatic metabolism of these agents (6). The role of mEH in xenobiotic detoxification is further supported by recent polymorphism studies showing a relationship between this enzyme and the susceptibility to emphysema (7), several forms of cancer (8–10), and Crohn's disease (11). Furthermore, mEH single nucleotide polymorphisms (SNPs) with high activity appear to enhance

the susceptibility to air pollution, leading to an increase in the risk of asthma (12). Potent inhibitors could be useful pharmacological tools to generate chemical knockouts of the enzyme to evaluate its role in xenobiotic metabolism.

Despite the fact that mEH knockout mice do not present an obvious phenotype (5), there are several new lines of evidence suggesting an endogenous role for this enzyme. A potential role of mEH in sexual development is supported by the facts that androstene oxide is a very good mEH substrate (1) and mEH is an apparent subunit of the antiestrogen-binding site (13). Such a role could be associated with the relationship between mEH polymorphism and spontaneous abortion (14) or preeclampsia (15). Furthermore, mEH is significantly expressed in ovaries, particularly in the follicle cells (1, 16). The mEH is also highly expressed in the adrenal gland (17). Alternatively, over the past decade, mEH has also been described as mediating the transport of bile acid in the liver (18). The mechanism by which mEH participates in this transport is not known. Obtaining potent mEH inhibitors will provide new tools to better understand the multiple roles of this enzyme.

We recently demonstrated that fatty amides, such as elaidamide **1**, represent a new class of potent inhibitors of mEH (19). While this compound is very active on recombinant mEH *in vitro*, with a  $K_i$  in the high nanomolar range, it is rapidly destroyed when incubated with liver microsomes (Figure 1). Incubation with 1,1,1-trifluoro-3-octylsulfanyl-propan-2-one (OTFP) significantly reduced the destruction of elaidamide **1**. OTFP is an inhibitor of carboxylesterases (20) but also of amidases such as fatty acid amide hydrolase (21), an enzyme able to hydrolyze amides to acids (22). Because only the amide function has inhibitory activity on mEH (19), the action of amidases results in a rapid loss of inhibition potency and makes

\* To whom correspondence should be addressed. Tel.: 530-752-7519. Fax: 530-752-1537. E-mail: bdhammock@ucdavis.edu.

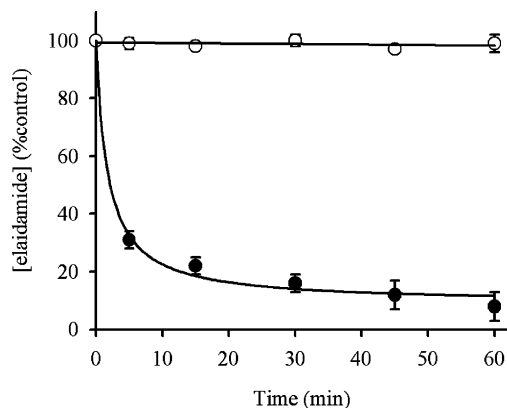
<sup>†</sup> Department of Entomology and UCD Cancer Center.

<sup>‡</sup> Present address: Western Human Nutrition Research Center, Agricultural Research Service, U.S. Department of Agriculture, University of California, Davis.

<sup>§</sup> Present address: Division of Physiological Chemistry 2, Department of Medical Biochemistry and Biophysics, Karolinska Institutet, 17177 Stockholm, Sweden.

<sup>||</sup> Department of Molecular Biosciences, School of Veterinary Medicine.

<sup>1</sup> Abbreviations: mEH, microsomal epoxide hydrolase; SNP, single nucleotide polymorphism; OTFP, 1,1,1-trifluoro-3-octylsulfanyl-propan-2-one; NSPA, 2-nonylsulfanyl-propionamide; *c*SO, *cis*-stilbene oxide; ESI-MS, electrospray ionization mass spectrometry; PMSF, phenylmethanesulfonyl fluoride; BSA, bovine serum albumin.



**Figure 1.** Stability of elaidamide **1**. One hundred micromolar **1** was incubated at 37 °C with rat liver microsomes (0.2 mg/mL) in the absence (●) or presence (○) of 100 μM OTFP. The remaining concentrations of **1** were determined over time by gas chromatography.

compounds like **1** unusable with crude extracts or in vivo. Therefore, the objective of this study was to design more metabolically stable mEH inhibitors by investigating the effect of structural changes on mEH inhibition and microsomal stability. The effect of these new inhibitors on naphthalene metabolism in isolated murine airways was also explored.

### Experimental Procedures

**Animals.** Male Swiss Webster mice were obtained from Harlan (San Diego, CA) and were maintained in HEPA-filtered cage racks at the University of California Davis vivarium for at least 5 days before use. The animals were housed under environmentally controlled conditions (0700–1900 h light cycle; 22–25 °C temperature). They were fed standard mouse chow (Purina Corp.) and water ad libitum, and the use of any pesticides or other xenobiotics was prohibited in the animal rooms for the duration of their stay. Animal care protocols and experimental procedures were approved by the University of California at Davis Institutional Animal Care and Use Committee.

**Chemicals and Apparatus.** Chemicals and reagents were obtained from Sigma (St. Louis, MO), Aldrich (Milwaukee, WI), or Nu-Chek-Prep (Elysian, MN). HPLC quality solvents were obtained from Fisher Scientific (Pittsburgh, PA) and used without further purification. Compound **8** was obtained from Alfa-Aesar (Ward Hill, MA), and compound **30** was obtained from Aldrich. Melting points (mp) were measured with a Thomas-Hoover apparatus (A. H. Thomas Co., Philadelphia, PA) and are uncorrected. <sup>1</sup>H and/or <sup>13</sup>C NMR were performed on a Mercury 300 NMR (Varian; Walnut Creek, CA). Gas chromatography–mass spectrometry (GC-MS) was performed on a Hewlett-Packard 6890 gas chromatograph (San Jose, CA) equipped with a 30 m × 0.25 mm × 0.25 μm film DB-5 ms (J&W Scientific, Folsom CA), and a 5973 mass spectral detector. electrospray ionization mass spectrometry (ESI-MS) was performed in positive mode on a Fisons Quattro BQ (Altrancham, England), 5 μL/min flow of 1:1:0.05 (v:v:v) acetonitrile:water:formic acid, and cone voltage of 50 V.

**Synthesis.** Inhibitor structures are given in tables, and boldface numbers throughout the text refer to these compounds. Compounds **1**, **2**, **11**, **22**, and **25** were synthesized previously in the laboratory (19, 23). Compounds **3–7**, **9**, **12**, **14**, **31**, and **32** were synthesized as previously published (24–26). The synthesis and characterization of other compounds used in this paper are given in Supporting Information. The chemical purity was estimated at >97% for each compound based on <sup>1</sup>H NMR spectra and ESI-LC/MS analyses. As an example, the synthesis of compound **16** is described below.

**2-Nonylsulfanyl-propionamide (NSPA, 16).** To a stirred solution of 0.76 g (5 mmol) of 2-bromo-propionamide, 0.8 g (5.2 mmol) of 1,8-diazabicyclo[5.4.0]undec-7-ene, and 5.0 mmol of potassium carbonate in 50 mL of ethyl acetate was added 1.2 g (5.0 mmol)

of 1-nonanethiol dissolved in 3 mL of ethyl acetate. The reaction was refluxed for 6 h. The solvent was evaporated under vacuum, and the residue was dissolved in 100 mL of a 97:3 mixture of hexane:ethyl acetate. The residue was purified by chromatography on a silica column (1 cm × 20 cm). The target compound (0.21 g, 20% yield) was eluted with a 80:20 mixture of hexane:ethyl acetate. The melting point of the resulting white powder was 68.0–69.0 °C. GC-MS *m/z* (relative intensity): 231 {3%, [M]<sup>+</sup> (C<sub>12</sub>H<sub>25</sub>NOS)}; 187 (10%, [M - CHNO]<sup>+</sup>); 159 (5%, [M - C<sub>3</sub>H<sub>6</sub>NO]<sup>+</sup>); 105 (2%, [M - C<sub>9</sub>H<sub>19</sub>]<sup>+</sup>); 73 (100%, [M - C<sub>9</sub>H<sub>18</sub>S]<sup>+</sup>). <sup>1</sup>H NMR (CDCl<sub>3</sub>, TMS): δ 6.62 (bd, *J* = 87.3 Hz, 1H, NH), 5.69 (bd, *J* = 54.6 Hz, 1H, NH), 3.37 (dd, *J* = 7.2 Hz, 1H, C2), 2.56 (t, *J* = 7.2 Hz, 2H, C4), 1.57 (m, 2H, C5), 1.47 (d, *J* = 7.8 Hz, 3H, methyl on C2), 1.25–1.40 (m, 12H, C6–11), 0.87 (t, *J* = 7.2 Hz, 3H, C12) ppm. <sup>13</sup>C NMR (CDCl<sub>3</sub>): δ 175.8 (C=O), 44.11 (C2), 31.83 (C10), 31.66 (C4), 28.89 (C6), 29.16 (C7), 29.22 (C8), 29.28 (C9), 29.43 (C5), 22.65 (C11), 18.51 (methyl on C2), 14.11 (C12) ppm. Anal. (C<sub>12</sub>H<sub>25</sub>NOS) theoretical: C, 62.29; H, 10.89; N, 6.05; S, 13.86%. Found: C, 62.32; H, 10.85; N, 6.08; S, 13.91%.

**Enzyme Preparation.** Recombinant rat mEH (RmEH) was produced in a baculovirus expression system as described (19). High Five insect cell cultures (derived from *Trichoplusia ni*; Invitrogen, San Diego, CA) were infected with the appropriate recombinant baculovirus at a multiplicity of infection of 0.1 virus per cell. After 80–84 h of incubation at 28 °C, cells were harvested by centrifugation (100g for 10 min at 4 °C). After suspension in chilled Tris/HCl buffer (0.1 M, pH 9.0) containing 1 mM phenylmethanesulfonyl fluoride (PMSF), EDTA, DTT, and 1% Lubrol PX, cells were disrupted using a Polytron homogenizer (9000 rpm for 60 s). The homogenate was centrifuged at 12000g for 20 min at 4 °C. The supernatant (crude extract) containing the mEH activity was frozen at –80 °C until used for the determination of IC<sub>50</sub> values. Protein concentrations were determined using the Bio-Rad Coomassie assay using Fraction V bovine serum albumin (BSA) as the calibrating standard.

**IC<sub>50</sub> Assay Conditions.** IC<sub>50</sub> values were determined using [<sup>3</sup>H]-*cis*-stilbene oxide (cSO) as the substrate (27). The enzyme (1 nmol min<sup>-1</sup> mL<sup>-1</sup>) was incubated with inhibitors for 5 min in Tris/HCl buffer (0.1 M, pH 9.0) containing 0.1 mg/mL BSA at 30 °C before substrate introduction ([S]<sub>final</sub> = 50 μM). After 5 min, the reaction was quenched by addition of 250 μL of isoactane, which extracted the remaining epoxide from the aqueous phase. The activity was followed by measuring the quantity of radioactive diol formed in the aqueous phase using a liquid scintillation counter (Wallac model 1409, Gaithersburg, MD). Assays were performed in triplicate. By definition, an IC<sub>50</sub> is the concentration of inhibitor that reduces enzyme activity by 50%. IC<sub>50</sub> values were determined by regression of at least five datum points in the linear region of the curve on either side of the IC<sub>50</sub>. The curve was generated from at least three separate runs, each in triplicate, to obtain the standard deviation (SD) in tables.

**Enzyme Purification.** Recombinant rat mEH (RmEH) was purified for the determination of dissociation constants, using a method modified from Lacouciere et al. (28). Insect cell cultures were infected and collected as indicated above. After suspension in chilled sodium phosphate buffer (0.1 M pH 7.4) containing 1 mM PMSF, EDTA, and DTT, cells were disrupted using a Polytron homogenizer (9000 rpm for 60 s). The homogenate was centrifuged at 100000g for 60 min at 4 °C. The pellet containing the targeted enzyme activity was then suspended in chilled Tris/HCl buffer (10 mM, pH 7.6, buffer A) containing 1% Tween 20. The homogenate was then centrifuged at 100000g for 60 min at 4 °C. The pellet was then suspended in chilled buffer A containing 1% Triton X-100 and centrifuged at 100000g for 60 min at 4 °C. The supernatant was dialyzed overnight against Tris/HCl buffer (10 mM pH 9.0) containing 0.05% of Lubrol PX (buffer B). The dialysate was poured on a 10 cm × 2.5 cm Q-Sepharose column equilibrated with buffer B. The column was washed with buffer B containing 25 mM NaCl. The targeted enzyme activity was eluted with buffer B containing 50 mM NaCl. The pooled active fractions were concentrated using Centriprep 50 (Amicon) and then dialyzed

against buffer A containing 0.05% of Lubrol PX. On average, purification yielded 20 mg of protein from 1 L of culture (~40% yield) with a specific activity around 250 nmol min<sup>-1</sup> mg<sup>-1</sup>. The preparations were at least 95% pure as judged by sodium dodecyl sulfate–polyacrylamide gel electrophoresis and scanning densitometry. The purified enzyme lost all activity if frozen but remained stable if stored at 4 °C (less than 10% activity loss over a 3 month period). Therefore, the enzyme preparation was kept in the refrigerator at 4 °C until use.

**Kinetic Assay Conditions.** Dissociation constants were determined using purified enzyme and *c*SO as substrate (27). Final inhibitor concentrations between 0 and 1000 nM for **1**, 0 and 150 nM for **16**, and 0 and 300 nM for **29** were used. The inhibitors were incubated with the purified RmEH (10 nM; 1 nmol min<sup>-1</sup> mL<sup>-1</sup>) for 5 min in 100  $\mu$ L of Tris/HCl buffer (0.1 M, pH 9.0) containing 0.1 mg/mL BSA at 30 °C. Reactions were performed in triplicate. Substrate (1.5 < [S]<sub>final</sub> < 50  $\mu$ M) was then added. The velocity was measured as described under IC<sub>50</sub> assay conditions. For each inhibitor concentration, the plots of the velocity as a function of the substrate concentration allowed the determination of apparent kinetic constants ( $K_{Mapp}$  and  $V_M$ ) (29). Resolution of the nonlinear Michaelis equation was performed using Sigma Plot (SPSS Science; Chicago, IL). The plot of  $K_{Mapp}$  as a function of the inhibitor concentration allowed the determination of  $K_I$ . Results are reported as means  $\pm$  SDs of three independent determinations of  $K_I$ .

**Microsomal Incubations.** Rat liver microsomes obtained previously in the laboratory (30) were diluted to ~0.2 mg/mL protein in potassium phosphate buffer (0.1 M, pH 7.4). To 930  $\mu$ L of microsomal preparation, 10  $\mu$ L of ethanol or 10 mM solution in ethanol of OTFP ([I]<sub>final</sub>, 100  $\mu$ M) was added. The mixture was incubated at 37 °C for 5 min before the addition of 10  $\mu$ L of 10 mM solution of **1**, **16**, or **29** in DMSO ([I]<sub>final</sub>, 100  $\mu$ M) and 50  $\mu$ L of buffer or NADPH generating system (31). This mixture was then incubated at 37 °C. At various time points (between 0 and 120 min), 100  $\mu$ L aliquots were removed and 1  $\mu$ L of 5 mM oleynitrile was added as an internal standard. These aliquots were then extracted using 500  $\mu$ L of ice-cold chloroform after vortexing and centrifugation at 4000g for 5 min. The organic phase was separated and dried under nitrogen. The residue was then reconstituted in 25  $\mu$ L of chloroform, 2  $\mu$ L of which was used for analysis. Gas chromatography with flame ionization detection (FID) was used to determine the concentration of **1**, **16**, and **29**. The system used was a Hewlett-Packard (HP) 5890A (San Jose, CA) equipped with a 30 m  $\times$  0.25 mm DB-17 capillary column (J&W Scientific, Folsom, CA). The initial oven temperature of 140 °C was held for 3 min and ramped at 20 °C/min to 250 °C and maintained for 1 min. The inlet and detector temperatures were 280 °C for both. Helium was used as the carrier gas at a flow of 1 mL/min at 200 °C. Calibration curves for **1**, **16**, or **29** contained six points from 0.3 to 100.0  $\mu$ M and were linear ( $r^2 > 0.99$ ).

**Naphthalene Metabolism in Mouse Liver Microsomes.** Mouse liver microsomes were prepared by differential centrifugation according to previously published methods (32). The protein concentration of the extract was adjusted to 1 mg/mL. The extract was incubated with a NADPH generating system (31) and 100  $\mu$ M naphthalene with or without 100  $\mu$ M **16** at 37 °C for 15 min. The reactions were stopped by placing them on ice. Naphthalene metabolites were recovered by solid phase extraction (32) and analyzed by reverse phase HPLC with UV detection (33).

**Naphthalene Metabolism in Situ in Mouse Airways.** Mice (three per group) were euthanized with an overdose of pentobarbital, and the trachea were isolated and cannulated as described earlier (34). The chest cavity was opened by midline sternotomy; both lungs and trachea were removed intact from the animal. This cannulated preparation was then used for naphthalene exposure and metabolic evaluation. Following perfusion of the parenchyma with agarose and brief (10 min) incubation in ice-cold medium [deficient Waymouth's MB 752/1 medium (without reduced glutathione, L-cysteine, L-cystine, L-glutamine, and L-methionine), from Gibco-BRL Laboratories, Grand Island, NY], incubation medium contain-

ing 100  $\mu$ M naphthalene was instilled into the tracheobronchial tree with or without 100  $\mu$ M **16**. Lungs were incubated at 37 °C for 60 min, and the incubation medium was then aspirated for analysis of naphthalene metabolites (33).

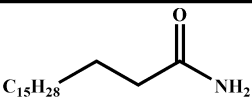
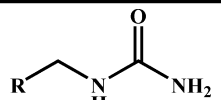
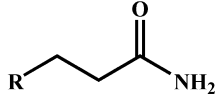
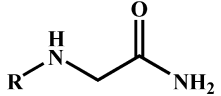
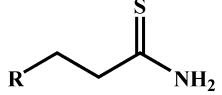
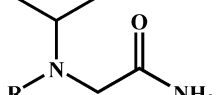
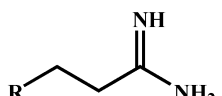
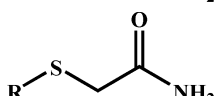
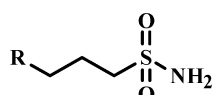
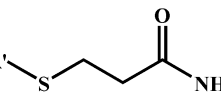
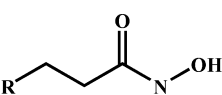
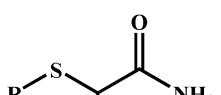
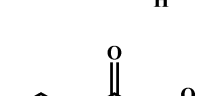
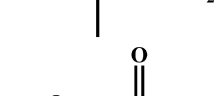
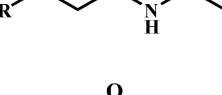
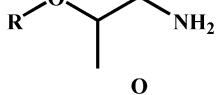
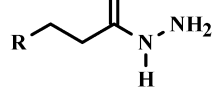
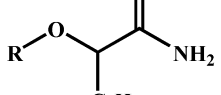
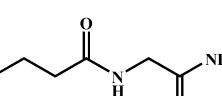
## Results

**Structure Optimization.** In a preliminary study, we identified primary amines and amides as good mEH inhibitors (19). While amines are toxic for cells in culture (data not shown), amides generally are much less toxic but are rapidly degraded (Figure 1). To obtain more stable and less toxic mEH inhibitors, we at first explored the effect of variation in the terminal function on the inhibition of rat mEH (Table 1). As compared to compound **2**, the replacement of the amide function by a thioamide **3**, guanidine **4**, or methyl-sulfonamide **5** reduced significantly the inhibitory potency. These data are consistent with results obtained for the soluble epoxide hydrolase (35). As compared to **2**, the presence of a hydroxyl **6**, methoxy **7**, amine **8**, or glycinamide **9** also reduced inhibition potency. These findings are consistent with previous results showing that best inhibition was obtained for primary amides (19). The presence of a methyl  $\alpha$  to the carbonyl in compound **10** resulted in a 2.5-fold increase in inhibition potency. As compared to the monosubstituted urea **11**, the movement of the substituted nitrogen to a  $\beta$ -position **12** resulted in a loss of inhibitory potency. Replacing the hydrogen on this nitrogen by an isopropyl **13** produced an inhibitory potency similar to **11**. This finding is consistent with a hydrophobic nature for the mEH active site. A hydrophobic active site has been suggested for mEH based on its substrate selectivity (2). Interestingly, the replacement of this nitrogen by a sulfur atom at the  $\beta$ -position **14** resulted in a 1 order of magnitude increase in inhibition potency, while this effect decreased 3-fold if the sulfur atom was placed at the  $\gamma$ -position as in **15**. The presence of a methyl at the  $\alpha$ -position and sulfur at the  $\beta$ -position (**16**) had an additional effect on the inhibition and yielded a 6-fold increase in potency. As compared to **16**, the replacement of the sulfur by oxygen **17** or a hydroxyl **19** in the  $\beta$ -position resulted in a substantial loss of potency. There was very little difference in potency between the presence of a methyl **17** or a phenyl **19** group at the  $\alpha$ -position.

To further optimize the inhibition of mEH activity by structural alteration, we then investigated the presence of several functions in the middle of the chain of elaidamide **1** (Table 2). We tried several oxidized functions of the olefin, **20–25**. Interestingly, each of these compounds gave a 2–4-fold increase in inhibitory potency, with the best obtained for the monohydroxyl, **24**. The replacement by a secondary amide function (**26**) resulted in a 1 order of magnitude loss of inhibition potency. A 4-fold recovery in potency was obtained when the hydrogen of the amide was replaced with an isopropyl group (**27**), underlining the hydrophobic nature of the binding site of the mEH. We then investigated the effect of the hydroxyl group position relative to the amide function (Table 3). There was basically no difference between position nine of **28** or 10 of **29**, but inhibition potency was significantly reduced when the hydroxyl was at position 12 of **30**. As compared to **30**, the presence of a double bond at position nine increased the inhibition potency; interestingly, similar results were obtained with a *cis*-**31** or *trans*-**32** olefin.

**Mechanism of Inhibition.** To understand the mode of action of these inhibitors, we determined the kinetic constants of inhibition for compounds **1**, **16**, and **29** with the purified rat mEH. As shown in Figure 2 for **16**, the data obtained fit a competitive model very well for all three inhibitors tested. We obtained an average ( $n = 3$ )  $K_I$  of  $430 \pm 70$ ,  $72 \pm 5$ , and 118

Table 1. Effect of the Terminal Function on the Inhibition of mEH

Structure <sup>a</sup>	IC <sub>50</sub> (μM) <sup>b</sup>	Structure	IC <sub>50</sub> (μM)		
	1	1.3 ± 0.1		11	12 ± 1
	2	2.34 ± 0.05		12	> 100
	3	> 100		13	14.1 ± 0.3
	4	13.2 ± 0.4		14	1.60 ± 0.01
	5	> 100		15	5.4 ± 0.1
	6	8.4 ± 0.4		16	0.39 ± 0.01
	7	> 100		17	6.1 ± 0.6
	8	> 100		18	8.2 ± 0.6
	9	> 100		19	14 ± 2
	10	0.93 ± 0.02			

<sup>a</sup> With R, *n*-C<sub>9</sub>H<sub>19</sub>; and R', *n*-C<sub>8</sub>H<sub>17</sub>. <sup>b</sup> The rat mEH and the inhibitors were incubated together for 5 min at 30 °C before the addition of substrate (cSO, 50 μM). Results are means ± SD of three separate experiments.


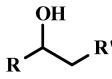
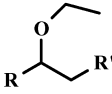
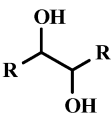
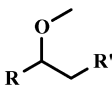
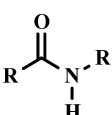
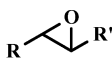
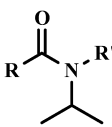
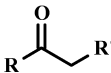
± 8 nM for **1**, **16**, and **29**, respectively, and  $r^2 \geq 0.98$ . The concentration of enzyme used in the kinetic assay is around 10 nM. For the best inhibitor **16**, the  $K_1$  is only 7-fold the estimated enzyme concentration, indicating a fairly tight association between the enzyme and this inhibitor. Interestingly, using a crude recombinant rat mEH, we previously found that **1** follows a linear mixed type inhibition, which is a mixture of competitive inhibition and noncompetitive inhibition (19). The presence of other proteins influences the activity of mEH (36). Therefore, one could postulate that in the crude mixture used previously, interaction with other proteins changed the apparent  $K_1$  and mode of inhibition. Noting the similarities in the sEH and mEH catalytic mechanisms (37) and the fact that ureas and amides are competitive inhibitors of the sEH (35), one would expect a competitive inhibition of mEH by amides as observed.

**Microsomal Stability.** To evaluate if, beyond improving inhibitor potency, the structural modifications improve the

metabolic stability of inhibitor described herein, we determined the half-life of **1**, **16**, and **29** in rat liver microsomal preparations in the presence or absence of OTFP and NADPH (Table 4). For all of the compounds studied, the addition of OTFP (an inhibitor of esterases and amidases (20, 21) that to our knowledge does not affect any other enzyme activity) increased their half-life substantially, underlying the susceptibility of these compounds to amide hydrolysis, especially for **1** and **29**. While the activation of P450 and flavin-dependent monooxygenases through the addition of NADPH reduced the half-life of all three compounds, the action of these enzymes seems more detrimental on **16**. In the conditions closest to physiologic (no OTFP but active P450s and flavin-dependent monooxygenases), the half-life of compound **16** is ~4-fold longer than that of **1** and **29**. Thus, the amide **16** was selected for further investigation.

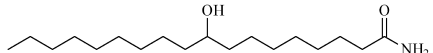
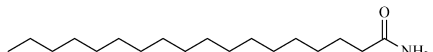
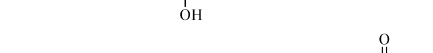
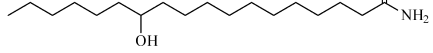
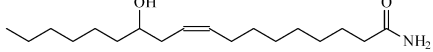
**Influence on Naphthalene Metabolism.** To test the efficacy of **16** to inhibit the mEH, we tested its ability to influence

Table 2. Effect of the Middle Chain Function on the Inhibition of mEH

Structure <sup>a</sup>	IC <sub>50</sub> (μM) <sup>b</sup>	Structure	IC <sub>50</sub> (μM)
	1 1.3 ± 0.1		24 0.31 ± 0.01
	20 0.67 ± 0.01		25 0.60 ± 0.04
	21 0.47 ± 0.01		26 26.7 ± 0.5
	22 0.38 ± 0.01		27 5.4 ± 0.1
	23 0.41 ± 0.01		

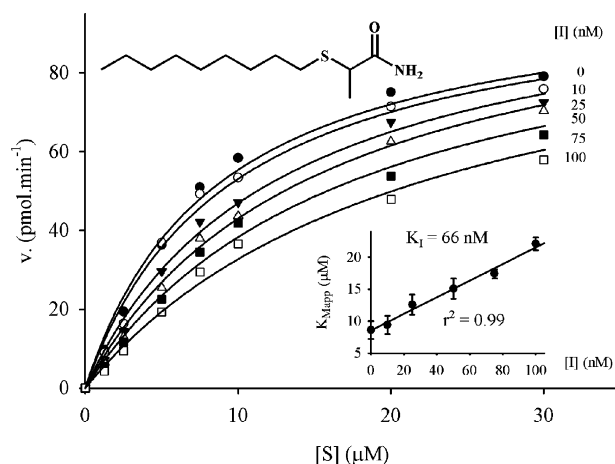
<sup>a</sup> With R, C<sub>8</sub>H<sub>17</sub>; and R', (CH<sub>2</sub>)<sub>7</sub>CONH<sub>2</sub>. <sup>b</sup> The rat mEH and the inhibitors were incubated together for 5 min at 30 °C before the addition of substrate (cSO, 50 μM). Results are means ± SD of three separate experiments.

Table 3. Effect of the Position of the Hydroxyl Function on mEH Inhibition

Structure	IC <sub>50</sub> (μM) <sup>a</sup>
	28 0.32 ± 0.01
	29 0.35 ± 0.01
	30 0.48 ± 0.03
	31 0.42 ± 0.01
	32 0.42 ± 0.02

<sup>a</sup> The rat mEH and the inhibitors were incubated together for 5 min at 30 °C before the addition of substrate (cSO, 50 μM). Results are means ± SD of three separate experiments.

naphthalene metabolism (Figure 3). Initially, we used mouse liver microsomes. In the presence of NADPH, naphthalene 1,2-oxide is formed, which is then hydrolyzed by mEH to yield a 1,2-dihydroxy-1,2-dihydronaphthalene or is chemically degraded to naphthol (33). While not influencing the naphthalene 1,2-oxide production, the addition of 100 μM **16** resulted in a 69 ± 2% decrease in 1,2-dihydroxy-1,2-dihydronaphthalene production and a ~2-fold increase in naphthol production, resulting in an overall 8-fold shift in naphthalene metabolism toward naphthol production. In a second series of experiments, we studied the effect of **16** on naphthalene metabolism in situ in mouse airways. Upon exposure to medium containing 100 μM **16**, we observed a 70 ± 17% decrease in 1,2-dihydroxy-1,2-dihydronaphthalene formation and a 70 ± 30% increase in naphthalene glutathione conjugates, suggesting that while naphthalene 1,2-oxide production was not significantly affected, its subsequent metabolism was shifted from the action of mEH to the action of GSTs. These data demonstrated the capacity of **16** to inhibit mEH in vitro and ex vivo.



**Figure 2.** Determination of  $K_i$  for compound **16** (NSPA) using [<sup>3</sup>H]-cSO as the substrate and purified rat mEH. For each concentration of inhibitor, the velocity is plotted as a function of substrate concentration, allowing the calculation of apparent Michaelis constants. In the insert, the  $K_{Mapp}$  values are plotted as a function of the inhibitor concentration, allowing the calculation of  $K_i$  (29). In the absence of inhibitor, a  $K_m$  of 8.6 ± 1.4 μM and a  $V_{max}$  of 107 ± 6 pmol min<sup>-1</sup> per assay were obtained for mEH hydrolysis of cSO.

Table 4. Microsomal Stability of Selected Inhibitors

	microsomal $t_{1/2}$ (min) <sup>a</sup>			
	-	+	-	+
OTFP	-	+	-	+
NADPH	-	-	+	+
<b>1</b>	2.1 ± 0.2	>120	1.5 ± 0.5	50 ± 3
<b>16</b>	26.0 ± 0.5	>120	8 ± 1	36 ± 5
<b>29</b>	2.8 ± 0.2	>120	1.5 ± 0.5	58 ± 4

<sup>a</sup> Each inhibitor (100 μM) was incubated at 37 °C with rat liver microsomes (0.2 mg/mL) in the absence or presence of 100 μM OTFP and NADPH generating system. The remaining concentrations of the inhibitor were determined over time by gas chromatography (see Figure 1 as typical results obtained). Results are means ± SD of three separate experiments.

## Discussion

Since its discovery 40 years ago (38), the mammalian mEH has been studied for its ability to metabolize epoxides formed

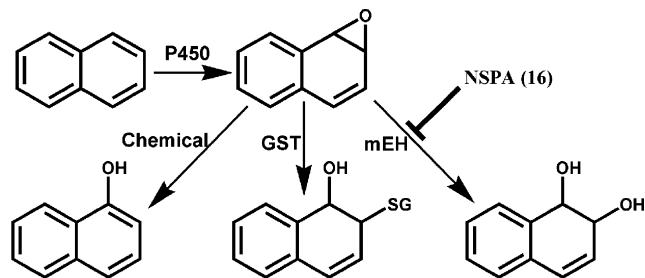


Figure 3. Naphthalene metabolism (33).

from numerous xenobiotics, such as polyaromatic hydrocarbons, 1,3-butadiene, phenytoin, and carbamazepine (1–3). While a few endogenous substrates have been reported for mEH, such as androstene oxide (16 $\alpha$ ,17 $\alpha$ -epoxyandrost-3-one), estroxiol (epoxyestratrienol), or epoxyfatty acids (1), the endogenous role of mEH is still unknown. Pharmacological inhibitors are classically used to probe the biologic role of an enzyme. A few years ago, we reported that fatty amides, such as elaidamide **1**, represent a new class of potent inhibitors of mEH (19). While this compound is very active on recombinant mEH in vitro, it is rapidly destroyed when incubated with liver microsomes (Figure 1). Herein, we investigated structural changes of **1** that could yield more potent and more stable mEH inhibitors. Improved inhibition (3.5-fold lower  $K_1$ ) is obtained when the olefin of **1** is replaced by a hydroxyl group **29**; however, the stability of the resulting compound was not improved. On the other end of the molecule, the addition of an  $\alpha$ -methyl group and a  $\beta$ -thio-ether function next to the amide carbonyl yielded a compound (**16**) that has a 6-fold lower  $K_1$  and is significantly more stable than **1**. Interestingly, for the inhibition of juvenile hormone esterase by trifluoroketones, an  $\alpha$ -methyl group and a  $\beta$ -thio-ether function next to the carbonyl also yield the most potent inhibitors (39). Finally, this new mEH inhibitor **16** significantly reduced the mEH-dependent production of 1,2-naphthalene diol in ex vivo lungs exposed to naphthalene, underlying the usefulness of the inhibitors described herein.

Because in most cases the resulting diols are less mutagenic or carcinogenic than the starting epoxide, mEH has an overall cytoprotective role by detoxifying xenobiotics. The protective role of mEH from xenobiotics is illustrated by the case of a man with a defect in mEH expression who suffered from acute and severe phenytoin toxicity (40). However, in the case of some polyaromatic compounds, such as benzo[ $\alpha$ ]pyrene or 7,12-dimethylbenz[ $\alpha$ ]anthracene (DMBA), dihydrodiol formation can stabilize the molecule after the formation of a second epoxide yielding highly mutagenic “diol epoxides” that can alkylate DNA while resisting further metabolism by mEH (4). This pro-carcinogenic role for mEH was documented in mEH knockout mice that were less sensitive to the carcinogenic activity of DMBA than control mice (5). Thus, “therapeutic” inhibition of the mEH enzyme could be viewed as either enhancing or reducing toxicity depending on the xenobiotic(s) involved. Valpromide or progabide treatments were found to increase the toxicity of carbamazepine or phenytoin (41), underlying the potential risks associated with the therapeutic inhibition of mEH. In addition, the genotoxicity of 1,3-butadiene, an important industrial chemical and common air pollutant, was found inversely correlated with predicted in vivo mEH activity (42). Thus, therapeutic inhibition of mEH could even be detrimental. However, the specter of intrinsic risk should not be generalized to all substrates transformed by mEH. In the case of polyaromatic air pollutants such as benzo[ $\alpha$ ]pyrene or 7,12-dimethylbenz[ $\alpha$ ]anthracene, the action of mEH leads to more

mutagenic and toxic metabolites (4, 5). A recent study showed that children with high predicted in vivo mEH activity have a 4-fold increased risk for lifetime asthma linked to polyaromatic air pollutant exposure (12). In this case, the therapeutic inhibition of mEH could be clinically beneficial.

Early metabolism studies in vitro showed that epoxides from xenobiotic olefins could be degraded by either glutathione-*S*-transferases (GST) or epoxide hydrolases (32, 43). However, the relative importance of each enzyme in vivo is not yet well-understood. In the case of aflatoxin B1, kinetic measurements and experimentation in rodents showed the predominance of GSTs for the detoxification of this chemical (44). However, more recent epidemiologic studies did not give clear answers about the relative importance of each enzyme (45, 46). Additionally, a recent microarray study suggests that resistance to the hepatotoxicity of bromobenzene in rats is mostly due to increased expression of GSTs and multidrug resistance protein 3 rather than mEH (47). For the metabolism of naphthalene in isolated lungs, we observed that the reduction of diol (70  $\pm$  17%) was accompanied by a similar increase (70  $\pm$  30%) in glutathione conjugates.

The metabolism of xenobiotics involves numerous enzymes and pathways. In most cases where mEH is involved, the inhibition of this hydrolase will likely be compensated by the action of other metabolizing enzymes, especially GST. In some cases, such metabolism shifts will increase and in a few cases decrease toxicity. The inhibitors developed herein should be viewed as valuable probes to investigate the physiological and biological roles of mEH and its relative importance to xenobiotic metabolism.

**Acknowledgment.** This work was partially funded by NIEHS Grants ES02710, ES04311, and ES04699; NIEHS Superfund Basic Research Program Grant P42 ES04699; and NIEHS Center for Environmental Health Sciences Grant P30 ES05707.

**Supporting Information Available:** Syntheses and detailed analytical data. This material is available free of charge via the Internet at <http://pubs.acs.org>.

## References

- (1) Newman, J. W., Morisseau, C., and Hammock, B. D. (2005) Epoxide hydrolases: Their roles and interactions with lipid metabolism. *Prog. Lipid Res.* 44, 1–51.
- (2) Wixtrom, R. N., and Hammock, B. D. (1985) Membrane-bound and soluble-fraction epoxide hydrolases: Methodological aspects. In *Biochemical Pharmacology and Toxicology, Vol. 1: Methodological Aspects of Drug Metabolizing Enzymes* (Zakim, D., and Vessey, D. A., Eds.) pp 1–93, John Wiley & Sons, Inc., New York.
- (3) Fretland, A. J., and Omiecinski, C. J. (2000) Epoxide hydrolases: Biochemistry and molecular biology. *Chem.-Biol. Interact.* 129, 41–59.
- (4) Szeliga, J., and Dipple, A. (1998) DNA adducts formation by polycyclic aromatic hydrocarbon dihydrodiol epoxides. *Chem. Res. Toxicol.* 11, 1–11.
- (5) Miyata, M., Kudo, G., Lee, Y.-H., Yang, T. J., Gelboin, H. V., Fernandez-Salguero, P., Kimura, S., and Gonzalez, F. J. (1999) Targeted disruption of the microsomal epoxide hydrolase gene: Microsomal epoxide hydrolase is required for the carcinogenic activity of 7,12-dimethylbenz[ $\alpha$ ]anthracene. *J. Biol. Chem.* 274, 23963–23968.
- (6) Zheng, J., Cho, M., Brennan, P., Chichester, C., Buckpitt, A. R., Jones, A. D., and Hammock, B. D. (1997) Evidence for quinone metabolites of naphthalene covalently bound to sulfur nucleophiles of proteins of mouse Clara cell after exposure to naphthalene. *Chem. Res. Toxicol.* 10, 1008–1014.
- (7) Smith, C. A. D., and Harrison, D. J. (1997) Association between polymorphism in gene for microsomal epoxide hydrolase and susceptibility to emphysema. *Lancet* 350, 630–633.
- (8) Kiyohara, C., Otsu, A., Shirakawa, T., Fukuda, S., and Hopkin, J. M. (2002) Genetic polymorphisms and lung cancer susceptibility: A review. *Lung Cancer* 37, 241–256.

- (9) To-figueras, J., Gené, M., Gómez-Catalán, J., Piqué, E., Borrego, N., Caballero, M., Cruellas, F., Raya, A., Dicenta, M., and Corbella, J. (2002) Microsomal epoxide hydrolase and glutathione S-transferase polymorphisms in relation to laryngeal carcinoma risk. *Cancer Lett.* 187, 95–101.
- (10) Baxter, S. W., Choong, D. Y. H., and Campbell, I. G. (2002) Microsomal epoxide hydrolase polymorphism and susceptibility to ovarian cancer. *Cancer Lett.* 177, 75–81.
- (11) De Jong, D. J., Van der Logt, E. M. J., Van Schaik, A., Roelofs, H. M. J., Peters, W. H. M., and Naber, T. H. J. (2003) Genetic polymorphisms in biotransformation enzymes in Crohn's disease: Association with microsomal epoxide hydrolase. *Gut* 52, 547–551.
- (12) Salam, M. T., Lin, P. C., Avol, E. L., Gauderman, W. J., and Gilliland, F. D. (2007) Microsomal epoxide hydrolase, glutathione S-transferase P1, traffic and childhood asthma. *Thorax* 62, 1050–1057.
- (13) Mésange, F., Sebbar, M., Kedjouar, B., Capdevielle, J., Guillemot, J.-C., Ferrara, P., Bayard, F., Delarue, F., Faye, J.-C., and Poirot, M. (1998) Microsomal epoxide hydrolase of rat liver is a subunit of the anti-oestrogen-binding site. *Biochem. J.* 334, 107–112.
- (14) Wang, X., Wang, M., Niu, T., Chen, C., and Xu, X. (1998) Microsomal epoxide hydrolase polymorphism and risk of spontaneous abortion. *Epidemiology* 9, 540–545.
- (15) Laasanen, J., Romppanen, E.-L., Hiltunen, M., Helisalmi, S., Mannermaa, A., Punnonen, K., and Heinonen, S. (2002) Two exonic single nucleotide polymorphisms in the microsomal epoxide hydrolase gene are jointly associated with preeclampsia. *Eur. J. Hum. Genet.* 10, 569–573.
- (16) Cannady, E. A., Dyer, C. A., Christian, P. J., Sipes, I. G., and Hoyer, P. B. (2002) Expression and activity of microsomal epoxide hydrolase in follicles isolated from mouse ovaries. *Toxicol. Sci.* 68, 24–31.
- (17) Coller, J. K., Fritz, P., Zanger, U. M., Siegle, I., Eichelbaum, M., Kroemer, H. K., and Mürdter, T. E. (2001) Distribution of microsomal epoxide hydrolase in humans: An immunohistochemical study in normal tissues, and benign and malignant tumours. *Histochem. J.* 33, 329–336.
- (18) Zhu, Q., Xing, W., Qian, B., von Dippe, P., Shneider, B. L., Fox, V. L., and Levy, D. (2003) Inhibition of human m-epoxide hydrolase gene expression in a case of hypercholanemia. *Biochem. Biophys. Acta* 1638, 208–216.
- (19) Morisseau, C., Newman, J. W., Dowdy, D. L., Goodrow, M. H., and Hammock, B. D. (2001) Inhibition of microsomal epoxide hydrolases by ureas, amides and amines. *Chem. Res. Toxicol.* 14, 409–415.
- (20) Wheelock, C. E., Severson, T. F., and Hammock, B. D. (2001) Synthesis of new carboxylesterase inhibitors and evaluation of potency and water solubility. *Chem. Res. Toxicol.* 14, 1563–1572.
- (21) Huang, H., Nishi, K., Tsai, H. J., and Hammock, B. D. (2007) Development of highly sensitive fluorescent assays for fatty acid amide hydrolase. *Anal. Biochem.* 363, 12–21.
- (22) Cravatt, B. F., Giang, D. K., Mayfield, S. P., Boger, D. L., Lerner, R. A., and Gilula, N. B. (1996) Molecular characterization of an enzyme that degrades neuromodulatory fatty-acid amides. *Nature* 384, 83–87.
- (23) Greene, J. F., Newman, J. W., Williamson, K. C., and Hammock, B. D. (2000) Toxicity of epoxy fatty acids and related compounds to cells expressing human soluble epoxide hydrolase. *Chem. Res. Toxicol.* 13, 217–226.
- (24) Applewhite, T. H., Nelson, J. S., and Goldblatt, L. A. (1963) Castor-based derivatives. Synthesis of some amides. *J. Am. Oil Chem. Soc.* 40, 101–104.
- (25) Drummond, J. T., and Johnson, G. (1988) Convenient procedure for the preparation of alkyl and aryl substituted N-(aminoalkyl)acyl-sulfonamides. *Tetrahedron Lett.* 29, 1653–1656.
- (26) Jones, P. B., Parrish, N. M., Houston, T. A., Stapon, A., Bansal, N. P., Dick, J. D., and Townsend, C. A. (2000) A new class of antituberculosis agents. *J. Med. Chem.* 43, 3304–3314.
- (27) Gill, S. S., Ota, K., and Hammock, B. D. (1983) Radiometric assays for mammalian epoxide hydrolases and glutathione S-transferase. *Anal. Biochem.* 131, 273–282.
- (28) Lacourcière, G. M., Vakharia, V. N., Tan, C. P., Morris, D. I., Edwards, G. H., Moos, M., and Armstrong, R. N. (1993) Interaction of hepatic microsomal epoxide hydrolase derived from a recombinant baculovirus expression system with a azarene oxide and an aziridine substrate analogue. *Biochemistry* 32, 2610–16.
- (29) Segel, I. H. (1993) *Enzyme Kinetics: Behavior and Analysis of Rapid Equilibrium and Steady-State Enzyme Systems*, John Wiley & Sons Inc., New York.
- (30) Morisseau, C., Derbel, M., Lane, T. R., Stoutamire, D., and Hammock, B. D. (1999) Differential induction of hepatic drug-metabolizing enzymes by fenvaleric acid in male rats. *Toxicol. Sci.* 52, 148–153.
- (31) Watanabe, T., and Hammock, B. D. (2001) Rapid determination of soluble epoxide hydrolase inhibitors in rat hepatic microsomes by high performance liquid chromatography with electrospray tandem mass spectrometry. *Anal. Biochem.* 299, 227–234.
- (32) Watt, K. C., Morin, D., Kurth, M. J., Mercer, R. S., Plopper, C. G., and Buckpitt, A. R. (1999) Glutathione conjugation of electrophilic metabolites of 1-nitronaphthalene in rat tracheobronchial airways and liver: identification by mass spectrometry and proton nuclear magnetic resonance spectrometry. *Chem. Res. Toxicol.* 12, 831–839.
- (33) Buckpitt, A. R., Chang, A. M., Weir, A., Van Winkle, L., Duan, X., Philpot, R., and Plopper, C. (1995) Relationship of cytochrome P450 activity to Clara cell. IV. Metabolism of naphthalene and naphthalene oxide in microdissected airways from mice, rats, and hamsters. *Mol. Pharmacol.* 47, 74–81.
- (34) Lin, C. Y., Isbell, M. A., Morin, D., Boland, B. C., Salemi, M. R., Jewel, W. T., Weir, A. J., Fanucchi, M. V., Baker, G. L., Plopper, C. G., and Buckpitt, A. R. (2005) Characterization of a structurally intact in situ lung model and comparison of naphthalene protein adducts generated in this model vs lung microsomes. *Chem. Res. Toxicol.* 18, 802–813.
- (35) Morisseau, C., Goodrow, M. H., Dowdy, D., Zheng, J., Greene, J. F., Sanborn, J. R., and Hammock, B. D. (1999) Potent urea and carbamate inhibitors of soluble epoxide hydrolases. *Proc. Natl. Acad. Sci. U.S.A.* 96, 8849–8854.
- (36) Ishii, Y., Takeda, S., Yamada, H., and Oguri, K. (2005) Functional protein-protein interaction of drug metabolizing enzymes. *Front. Biol.* 10, 887–895.
- (37) Morisseau, C., and Hammock, B. D. (2005) Epoxide hydrolases: Mechanisms, inhibitor designs, and biological roles. *Annu. Rev. Pharmacol. Toxicol.* 45, 311–333.
- (38) Jerina, D., Daly, J., Wiltkop, B., Zaltzman-Nirenberg, P., and Udenfriend, S. (1968) Role of the arene oxide-oxepin system in the metabolism of aromatic substrates. I. In vitro conversion of benzene oxide to a premercapturic acid and a dihydrodiol. *Arch. Biochem. Biophys.* 128, 176–183.
- (39) Linderman, R. J., Leazer, J., Venkatesh, K., and Roe, R. M. (1987) The inhibition of insect juvenile hormone esterase by trifluoromethylketones: Steric parameters at the active site. *Pestic. Biochem. Physiol.* 29, 266–277.
- (40) Yoo, J. H., Kang, D. S., Chun, W. H., Lee, W. J., and Lee, A. K. (1999) Anticonvulsant hypersensitivity syndrome with an epoxide hydrolase defect. *Br. J. Dermatol.* 140, 181–183.
- (41) Spina, E., Pisani, F., and Perucca, E. (1996) Clinically significant pharmacokinetic drug interactions with carbamazepine. An update. *Clin. Pharmacokinet.* 31, 198–214.
- (42) Abdel-Rahman, S. Z., Ammenheuser, M. M., Omiecinski, C. J., Wickliffe, J. K., Rosenblatt, J. I., and Ward, J. B. (2005) Variability in human sensitivity to 1,3-butadiene: Influence of polymorphisms in the 5'-flanking region of the microsomal epoxide hydrolase gene (EPHX1). *Toxicol. Sci.* 85, 624–631.
- (43) Siedegård, J., and Ekström, G. (1997) The role of human glutathione transferases and epoxide hydrolases in the metabolism of xenobiotics. *Environ. Health Perspect.* 105, 791–799.
- (44) Guengerich, F. P., Johnson, W. W., Shimada, T., Ueng, Y. F., Yamazaki, H., and Langouet, S. (1998) Activation and detoxication of aflatoxin B1. *Mutat. Res.* 402, 121–128.
- (45) Tiemersma, E. W., Omer, R. E., Bunchoten, A., van't Veer, P., Kok, F. J., Idris, M. O., Kadaru, A. M., Fedail, S. S., and Kampman, E. (2001) Role of genetic polymorphism of glutathione-S-transferase T1 and microsomal epoxide hydrolase in aflatoxin-associated hepatocellular carcinoma. *Cancer Epidemiol. Biomarkers Prev.* 10, 785–791.
- (46) Dash, B., Afriyie-Gyawu, E., Huebner, H. J., Porter, W., Wang, J. S., Jolly, P. E., and Phillips, T. D. (2007) Determinants of the variability of aflatoxin-albumin adduct levels in Ghanaians. *J. Toxicol. Environ. Health A* 70, 58–66.
- (47) Tanaka, K., Kiyosawa, N., Watanabe, K., and Manabe, S. (2007) Characterization of resistance to bromobenzene-induced hepatotoxicity by microarray. *J. Toxicol. Sci.* 32, 129–134.

TX700446U